(Online) ISSN 2712-0562
Sustainable Engineering and Innovation *Original Research*
Vol. 7, No. 1, 2025, pp.127-136
https://doi.org/10.37868/sei.v7i1.id454

Reconfigurable metasurface based on graphene optical antennas for dynamic beam steering

Zahraa J. Abdulkareem [1*], Tagreed K. Hamad[2], Taha A. Elwi[3]
[1,2] Laser and Optoelectronics Engineering, Al-Nahrain University, Iraq
[3] Information Engineering, Al-Nahrain University, Iraq

*Corresponding author E-mail: Zjabdulkareem@gmail.com

Received Jan. 3, 2025
Revised Mar. 2, 2025
Accepted Mar. 13, 2025
Online Mar. 15, 2025

Abstract

Metasurface represents a transformative advancement in photonics due to its exotic abilities to control electromagnetic wave properties. The integration of graphene and metasurface propels metasurface to new heights of compact footprint, reconfigurability, and multi-functionality. In this article, a reconfigurable metasurface based on graphene optical antennas is designed as a reflective surface that controls the beam steering by tuning graphene's Fermi energy based on the concept of a phase-shifting surface. The results demonstrated that the designed metasurface can dynamically steer the reflected beam at different reflection angles, in addition to their capability to reflect a single beam and three beams. The metasurface exhibits high gain and directivity at different reflection angles. These steering capabilities provide a potentially efficient method for developing and simplifying dynamic reconfigurable beam-steering systems.

Keywords: Reconfigurable metasurface, Graphene, Optical antennas, Beam steering, Fermi energy

1. Introduction

Beam steering technology is one of the most important topics in various applications, including light detection and ranging (LiDAR) [1,2], free-space communications [3,4], and imaging [5-7]. Optical beam steering involves dynamically forming or redirecting a collimated or focused light beam into a specific direction by altering the relative phase of a wave [8]. The requirement for beam steering technology with high directivity has grown in the infrared optics-based fields [9,10]. Conventional beam-steering techniques, including microelectromechanical systems (MEMS) [11], spatial light modulators (SLM) [12], and diffraction gratings [13] suffer from slow modulation speed, small beam-steering angle cause a narrow field-of-view (FOV), and environmental/temperature sensitivity [8,14].

In recent years, metasurfaces have emerged as innovative technology for accurate wavefront manipulation characterized by ultra-thin size and fast response [15]. Metasurface, the 2D counterpart of metamaterials, is an ultrathin optical component composed of subwavelength elements, known as optical antennas, designed with spatially varying structural characteristics [16,17]. By altering the geometry or material properties of this optical antenna, the metasurfaces create a spatial variation in the reflected or transmitted wave properties [18]. A key

feature of the metasurface is their ability to introduce abrupt phase discontinuities at the interface via engineering the interaction between wave and optical antenna, enabling precise control over the optical wavefront [19]. Thus, the metasurfaces are integrated with active materials or applied external stimuli such as electrical or optical signals [20,21]. They offer the benefit of reconfigurability and multifunctionality, making them suitable for various applications that demand real-time adaptivity [22-24]. Among these active materials, Graphene is a monolayer of carbon atoms organized in a two-dimensional hexagonal lattice structure [25]. Graphene attracted significant interest in the infrared and terahertz (THz) regimes since its Fermi energy and the corresponding surface conductivity can be tuned by applying a bias voltage [26]. Various reconfigurable metasurfaces based on graphene have been wildly proven to realize dynamic beam steering [27-30]. In the communication field, the primary function of dynamic beam steering is to expand the antenna coverage area so that many communication devices can be accommodated. It also reduces path interference by enhancing the gain and directivity of the antenna while reducing power consumption by directing the reflected beams (or transmitted signals) to only the desired direction. In addition, it provides security against non-intended users by controlling the properties of reflected beams through dynamic beam steering [31,32].

In this article, we propose a reconfigurable metasurface based on graphene optical antennas for dynamic beam steering. The modulation in the Fermi energy of graphene optical antennas enables the phase shift distribution required for beam steering. Therefore, the designed metasurface directs single- and triple-reflected beams in different directions. The performance of the designed metasurface is characterized by high gain and directivity. Thus, metasurface based on graphene optical antennas provides a promising reconfigurable platform for dynamic beam steering systems.

2. Research method

The schematic of the proposed metasurface based on graphene optical antennas is shown in Figure 1a. It consists of four layers: the top layer is graphene ribbons that act as optical antennas, which can be modulated to different Fermi energy (E_f), an interlayer of polydimethylsiloxane (PDMS), a gold layer acts as the back reflector, and a lower PDMS layer exhibits flexibility for structure. The corresponding sectional view for the designed metasurface is demonstrated in Fig. 1(b). The periodicity of the graphene antenna (P) is set as 1.7μm, and the width of each graphene antenna (W) is set as 1.6μm. The thickness (t_1) and refractive index of the PDMS interlayer are set as 0.8μm and 1.96, respectively. Beneath the PDMS layer, there is an optically thick gold layer with a thickness (t_2) of 1μm and a lower PDMS layer of 1μm thickness (t_3). This structure can provide the Fabry-Perot resonator in the PDMS spacing layer, in which the graphene antennas act as a partially reflecting mirror in the front, and the gold layer serves as the total reflecting mirror in the back.

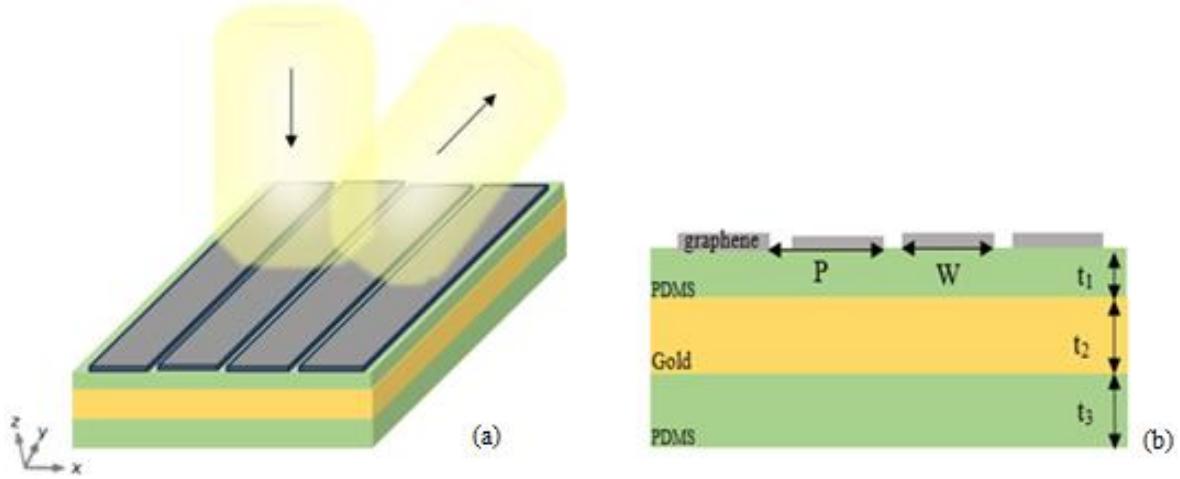

Figure 1. (a) Schematic and (b) The sectional view of the designed reconfigurable metasurface based on graphene optical antennas, respectively. P is antenna periodicity, W is graphene antenna width, t_2 is the thickness of the gold layer, and t_1 and t_3 are the thickness of the upper and lower PDMS layers

The electromagnetic response of graphene can be characterized by its surface conductivity (σ_g), which is composed of two main parts: the interband (σ_{inter}) and intraband (σ_{intra}) conductivities. The surface conductivity of graphene is described by the Kubo formula: $\sigma_g = \sigma_{intra} + \sigma_{inter}$. For the infrared regions, the surface conductivity of graphene that is dominated by the intraband transition can be derived by the semi-classical Drude model [33]:

$$\sigma(\omega) = \frac{i\, e^2 k_B}{\pi\, \hbar^2(\omega + i\tau^{-1})}\left[\frac{E_f}{k_B T} + 2ln\left(exp\left(\frac{-E_f}{k_B T}\right) + 1\right)\right] \quad (1)$$

where ω is the angular frequency, e is the electron charge, k_B is the Boltzmann constant, T is the temperature, $\hbar$ is the reduced Plank's constant. The carrier relaxation time can be calculated by $\tau = \mu\, E_f / e\, V_f^2$, where the carrier mobility (μ) is equal to $10^4 cm^2/V.s$ and the Fermi velocity (V_f) is equal to $10^6\ m/s$. The permittivity of graphene can be calculated from the equation: $\varepsilon_g = 1 + i\frac{\sigma_g(\omega)}{\omega t_g \varepsilon_0}$. Here, the ε_0 and t_g are the vacuum permittivity and the thickness of the graphene layer [34]. The Fermi energy of graphene can be expressed as $E_f = \hbar\, V_f \sqrt{\pi\, n_s}$, the graphene carrier density $n_s = \varepsilon_0 \varepsilon_d V_g / e\, d$, shows a linear dependence on the external gate voltage (V_g). Thus, the Fermi energy of the graphene antennas can be easily modulated by tuning the gate voltage [35]. We utilize the 2D Finite Element Method (FEM) to investigate the electromagnetic response of the proposed reconfigurable metasurface by COMSOL Multiphysics software. To reduce the difficulty of calculation, the finite graphene antenna thickness is replaced by the transition boundary condition, and the graphene conductivity is allocated to a single interface whose effective thickness is $t_g = 0.34\ nm$. The linearly polarized wave (λ=12.7 μm) is normally incident on the metasurface, and its polarization is parallel to the *x*-axis. Since the metasurface structure is constructed from the Fabry-Perot resonator (in interlayer PDMS) to enhance the reflected phase. Firstly, we examine the effect of PDMS interlayer thickness (t_1) on the reflectance and reflected phase at different the E_f values.

Figure 2a and 2b illustrate the reflectance and reflected phase map as a function of PDMS interlayer thickness and Fermi energy of the graphene antenna. A pronounced resonance feature is observed with an increase in t_1 and E_f value, causing a variation in the reflected amplitude and the phase. Figure 2b shows that the phase shift gradually increases with E_f and t_1 value, forming a stepped pattern due to the overlap between Fabry-Perot resonance and graphene plasmons, leading to a large accumulation of the phase shifts for 2π coverage that is required for full wavefront control [36]. When the E_f value above 0.72 eV and t_1 ~ 0.7–0.8μm, the phase shift reaches its maximum value equal to 350°, indicating a thicker PDMS layer (0.8μm) is a better option for phase modulation. Figure 2c and 2d show the reflectance and reflected phase shift of the metasurface with t_1=0.8 μm at different Fermi energies.

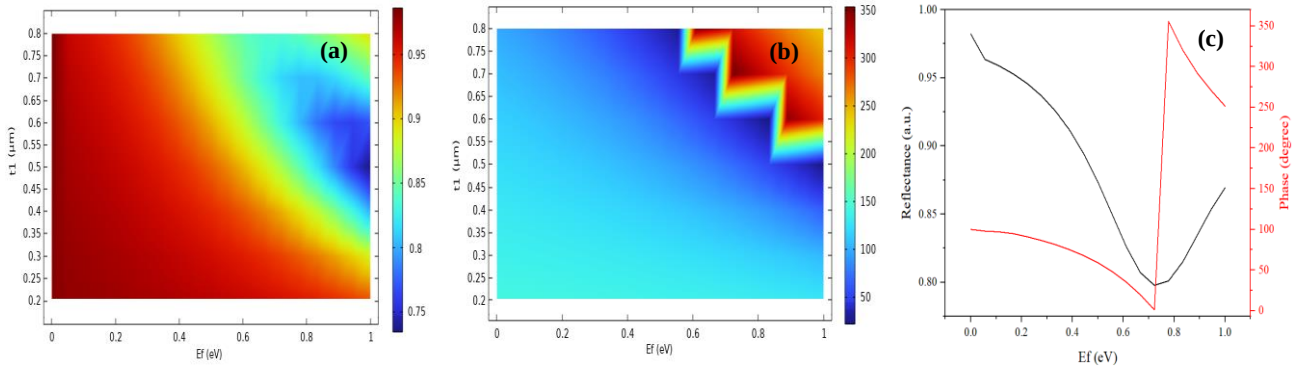

Figure 2. (a) Reflectance and (b) Phase shift map as a function of the Fermi energy and the PDMS thickness. (c) The reflectance and reflected phase shift of the metasurface as a function of the Fermi energy at t_1=0.8 μm

3. Results and discussion

The direction of the reflected beam can be steered by controlling the reflected phase per each graphene antenna. The desired phase gradient can be achieved by arranging the sequence of Fermi energy of the graphene antennas; thereby, the reflection angle becomes electrically reconfigurable. When the wave incidents normally on the metasurface, the reflection angle of the designed metasurface is calculated according to generalized Snell's law [29]:

$$\theta_r = \sin^{-1}\left(\frac{\lambda_0}{2\pi}\frac{d\Phi}{dx}\right) \quad (2)$$

where θ_r is the reflection angles, λ_0 is the wavelength, $d\Phi$ and dx represent the phase difference and geometric distance between adjacent graphene optical antennas. The designed metasurface is constructed with twenty graphene optical antennas. The Fermi energy corresponding to the phase between adjacent graphene antennas is obtained by applying the relationship between the Fermi energy and phase in Figure 2c. Thus, the metasurface was designed with the phase shift of 0º, 16º, -16º, and -29º between adjacent graphene ribbons to steer the beam with reflection angles 0º, 20º, -20º, and -37º, respectively. The simulated electric field E_x distribution demonstrated an anomalous reflection of the reflected wave in a single beam, as shown in Figure 3a-d. Figure 3f-h illustrates the distribution of phase shift and Fermi energy along the metasurface to achieve a reflected beam with different reflection angles. For a reflection angle of 20º, as shown in Figure 3f, the reflected phase varies significantly, especially in the first half of the metasurface, where multiple phase discontinuities appear due to variations in graphene's Fermi energy. The linear decline of Fermi energy suggests a controlled tuning for graphene conductivity, which affects the surface plasmon characteristics that interact with the incident beam to reflect it at an angle of 20º.

This distribution of a phase shift and Fermi energies are reversed along the metasurface to reflect the beam at an angle of -20º as demonstrated in Figure 3g. The phase response follows a complex variation to reflect the beam at an angle of -37º, showing discontinuities and jumps at specific points, as depicted in Figure 3h. The sharp phase transitions align with the points where the Fermi energy changes abruptly. Fermi energy forms a periodic triangular pattern with linear increases and sudden drops, which refers to the tuning of graphene conductivity along the metasurface. The abrupt phase changes with the tuning of graphene conductivity indicate that each graphene antenna of the metasurface acts as a localized phase shifter to reflect the beam at an angle of -37º.

To perform multi-beam steering for directional radiation, different phase shifts are introduced to the graphene antennas. Using the same twenty graphene antennas with changes the phase shift to ± 24º to reflect the wave at ±30º. Figure 3e shows the simulated electric field E_x distribution of three beams at reflection angles of -30º, 0º, 30º. The distribution of phase shift and Fermi energy along the metasurface is depicted in Figure 3i. The phase distribution curve exhibits three distinct phase gradient regions, each corresponding to a different spatial section of the metasurface. These controlled variations in the reflected phase allow for three separate reflection angles, meaning the wave is split into three beams instead of reflecting in a single direction. These phase gradients correspond to abrupt changes in Fermi energy, showing a direct relation between graphene's electrical tuning and phase modulation to reflect three beams at three different angles.

The performance of the designed metasurface based on graphene optical antennas is described by calculating the far-field radiation pattern and directivity of the reflected beam. Figure 4a-d demonstrates a far-field radiation pattern corresponding to the simulated electric field distribution in Figure 3. These results show a good agreement with the theoretical values of angles. In the far-field region, a single beam with a gain of 36dB, 35.8dB, and 34.9dB is observed at the direction of 0º, 20º, -20º, and -37º, respectively. The directivity value reaches 39.1dB, 37.5dB, and 35.26dB for a reflected beam with angles 0º, 20º, and -37º, respectively. The directivity is calculated according to the Kraus formula in [37]. The radiation pattern of the metasurface shows a high-directional beam with low distortions. The radiation pattern for multiple reflected beams with angles of -30º, 0º, 30º is illustrated in Figure 4e. The radiation pattern shows three beams with a gain of 27.6dB, 16dB, and 21dB and a directivity of 31dB, 23.4dB, and 28.1dB.

The dynamic redirecting of a collimated light beam into a specific direction or position by modulating the Fermi energy of graphene optical antennas enables reconfigurable optical systems for applications in infrared imaging, sensing, and wireless optical communications.

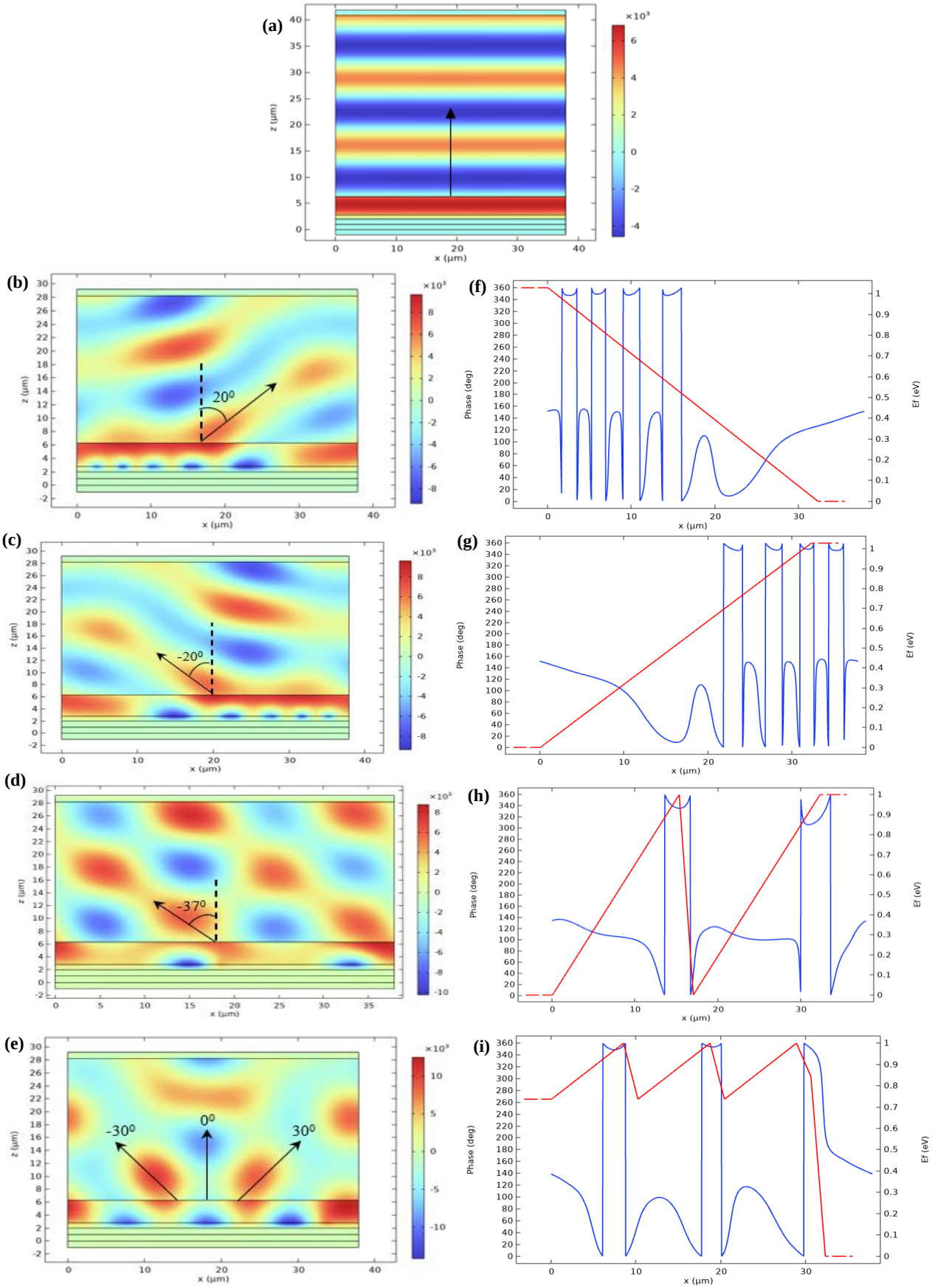

Figure 3. (a, b, c, d, e) Electric field distribution and (f, g, h, i) Distribution of the Fermi energy (red line) with the reflected phase (blue line) along the designed metasurface at 0º, 20º, -20º, -37º, and -30º 0º 30º.

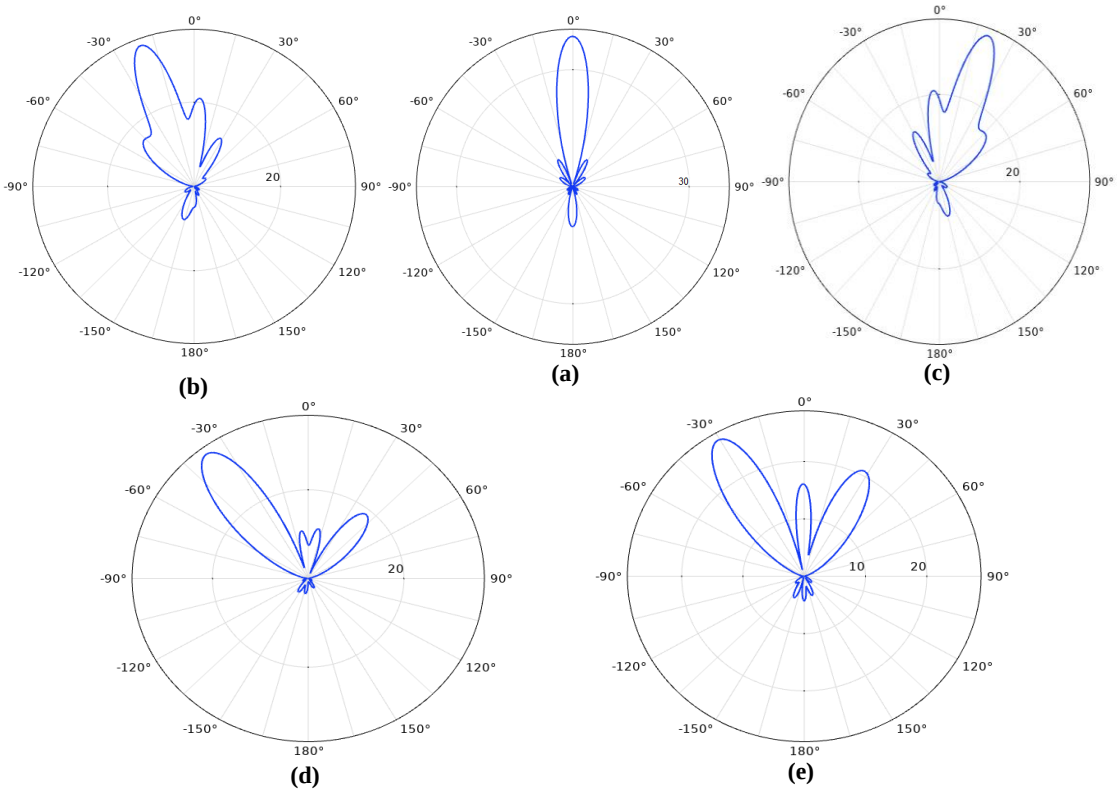

Figure 4. (a, b, c, d, e) The far-field radiation pattern of reflected beam at angles 0º, 20º, -20º, -37º, and -30º 0º 30º, respectively.

Table 1 compares the reconfigurable metasurface based on graphene optical antennas proposed in this work with previous studies.

Table 1. Comparison of the reconfigurable metasurface based on graphene antennas.

Ref.	Frequency (THz)	Reflectance	Steering angle	No. of beams	Gain (dB)	Directivity (dB)
[38]	5	0.59	0º-35º	Single	-	-
[39]	1.05	0.45	-5º,-11º,-17º,-23º	-	-	9.6
[40]	12.32	0.55	13º,-42º,42º	Single,double,triple	30.1	-
[41]	3-4	0.6	20.2º ,23.3º,27.4º	Single	-	-
Our work	23.6 (12.7µm)	0.82	0º,±20º, ±30º,37º	Single & triple	36	39.1

4. Conclusions

In summary, we have introduced and numerically investigated a reconfigurable metasurface based on graphene optical antennas for dynamic beam-steering function. The graphene antennas can introduce 350º phase modulation by tuning the graphene's Fermi energy. The simulation results demonstrated that the designed metasurface can dynamically steer the reflected beam with different reflection angles. The near-field distributions and the far-field radiation pattern show the metasurface capability to reflect a single beam and three beams. The performance of the designed metasurface is characterized by high gain and directivity with low distortion. Depending on the capability of the metasurface based on graphene antennas to perform dynamic beam steering, it provides superior solutions for multi-user indoor communications systems.

Declaration of competing interest

The authors declare that they have no known financial or non-financial competing interests in any material discussed in this paper.

Funding information

No funding was received from any financial organization to conduct this research.

Author contribution

Zahraa A. Abdulkareem: Methodology, Simulation, Data analysis, Investigation, Writing the manuscript, and interrupting the results. Tagreed K. Hamad and Taha A. Elwi: Review and supervision.

References

[1] C. Kyrou, R. Martins, E. Marinov, and P. Genevet, "Metasurfaces for light detection and ranging," Nanophotonics X, p. 23, 2024.

[2] I. Kim, R. J. Martins, J. Jang, T. Badloe, S. Khadir, H. Jung, H. Kim, J. Kim, P. Genevet, and J. Rho, "Nanophotonics for light detection and ranging technology," Nature Nanotechnology, vol. 16, no. 5, pp. 508–524, 2021.

[3] J. Tao, Q. You, C. Yang, Z. Li, L. Deng, M. Wu, M. Luo, L. Wu, C. Li, Z. Liu, Z. He, X. Xiao, G. Zheng, and S. Yu, "Beam-steering metasurfaces assisted coherent optical wireless multichannel communication system," Nanophotonics, vol. 12, no. 17, pp. 3511–3518, 2023.

[4] H. Taghvaee, A. Pitilakis, O. Tsilipakos, A. C. Tasolamprou, N. V. Kantartzis, M. Kafesaki, A. C. Aparicio, E. Alarc´on, and S. Abadal, "Multi-wideband Terahertz Communications Via Tunable Graphene-Based Metasurfaces in 6G Networks: Graphene Enables Ultimate Multiwideband THz Wavefront Control," IEEE Vehicular Technology Magazine, vol. 17, no. 2, pp. 16–25, 2022.

[5] K. Lindfors, D. Dregely, M. Lippitz, N. Engheta, M. Totzeck, and H. Giessen, "Imaging and Steering Unidirectional Emission from Nanoantenna Array Metasurfaces," ACS Photonics, vol. 3, no. 2, pp. 286–292, 2016.

[6] M. Raval, A. Yaacobi, and M. R. Watts, "Integrated visible light phased array system for autostereoscopic image projection," Optical Letter, vol. 43, pp.15, pp. 3678–3681, 2018.

[7] G. Yang, W. Han, T. Xie, and H. Xie, "Electronic holographic three-dimensional display with enlarged viewing angle using non-mechanical scanning technology," OSA Continuum, vol. 2, no. 6, p. 1917, 2019.

[8] P. Berini, "Optical Beam Steering Using Tunable Metasurfaces," ACS Photonics, vol. 9, no. 7, pp. 2204–2218, 2022.

[9] J. Midkiff, K. M. Yoo, J. D. Shin, H. Dalir, M. Teimourpour, and R. T. Chen, "Optical phased array beam steering in the mid-infrared on an InP-based platform," Optica, vol. 7, no. 11, p. 1544, 2020.

[10] S. I. Kim, J. Park, B. G. Jeong, D. Lee, K. Yang, Y. Park, K. Ha, and H. Choo, "Two-dimensional beam steering with tunable metasurface in infrared regime," Nanophotonics, vol. 11, no. 11, pp. 2719–2726, 2022.

[11] Y. Wang, G. Zhou, X. Zhang, K. Kwon, P. Blanche, N. Triesault, K. Yu, and M. C. Wu, "2D broadband beam steering with large-scale MEMS optical phased array," Optica, vol. 6, no. 5, p. 557, 2019.

[12] Z. He, F. Gou, R. Chen, K. Yin, T. Zhan, and S.-T. Wu, "Liquid Crystal Beam Steering Devices: Principles, Recent Advances, and Future Developments," Crystals, vol. 9, no. 6, p. 292, 2019.

[13] W.-B. Lee, C.-S. Im, C. Zhou, B. Bhandari, D.-Y. Choi, and S.-S. Lee, "Metasurface doublet-integrated bidirectional grating antenna enabling enhanced wavelength-tuned beam steering," Photonics Research, vol. 10, no. 1, p. 248, 2021.

[14] J. Tao, Q. You, Z. Li, L. Deng, M. Wu, M. Luo, L. Wu, R. Fu, Z. Liu, C. Yang, C. Li, Z. He, X. Xiao, G. Zheng, and S. Yu, "Beam-Steering Metadevices for Intelligent Optical Wireless-Broadcasting Communications," Advanced Photonics Research, vol. 4, no. 9, 2023.

[15] V. C. Su, C. H. Chu, G. Sun, and D. P. Tsai, "Advances in optical metasurfaces: fabrication and applications [Invited]," Optics Express, vol.26, no. 10, p.13148, 2018.

[16] E. Mikheeva, C. Kyrou, F. Bentata, S. Khadir, S. Cueff, and P. Genevet, "Space and Time Modulations of Light with Metasurfaces: Recent Progress and Future Prospects," ACS Photonics, vol. 9, no.5, pp.1458–1482, 2022.

[17] X. Wang, J. Ding, B. Zheng, S. An, G. Zhai, and H. Zhang, "Simultaneous Realization of Anomalous Reflection and Transmission at Two Frequencies using Bi-functional Metasurfaces," Scientific reports, vol.8, no.1, 2018.

[18] H. Zhou, J. Cheng, F. Fan, X. Wang, and S. Chang, "Graphene-based transmissive terahertz metalens with dynamic and fixed focusing," Journal of Physics D: Applied Physics, vol.53, no.2, p.025105, 2019.

[19] F. Ding, A. Pors, and S. I. Bozhevolnyi, "Gradient metasurfaces: a review of fundamentals and applications," Reports on Progress in Physics., vol.81, no.2, p.026401 2017.

[20] T. Cui, B. Bai, and H. Sun, "Tunable Metasurfaces Based on Active Materials," Advanced Functional Materials, vol.29, no.10, 2019.

[21] W. Luo, S. A. Abbasi, S. Zhu, X. Li, H.-P. Ho, and W. Yuan, "Electrically switchable and tunable infrared light modulator based on functional graphene metasurface," Nanophotonics, vol.12, no.9, pp.1797–1807, 2023.

[22] Z. Zhang, H. Shi, L. Wang, J. Chen, X. Chen, J. Yi, A. Zhang, and H. Liu, "Recent Advances in Reconfigurable Metasurfaces: Principle and Applications," Nanomaterials, vol.13, no.3, p.534, 2023.

[23] D. Neshev and I. Aharonovich, "Optical metasurfaces: new generation building blocks for multi-functional optics," Light: Science & Applications, vol. 7, no.1, 2018.

[24] F. Han, T. L. Pham, K. Pilarczyk, N. T. Tung, D. H. Le, G. A. E. Vandenbosch, J. V. de Vondel, N. Verellen, X. Zheng, and Ewald Janssens, "Tunable Mid-Infrared Multi-Resonant Graphene-Metal Hybrid Metasurfaces," Advanced optical materials, vol.12, no.19, 2024.

[25] C. Zeng,H. Lu, D. Mao, Y. Du, H. Hua, W. Zhao, and J. Zhao, "Graphene-empowered dynamic metasurfaces and metadevices," Opto-Electronic Advances, vol. 5, no. 4, pp.200098–200098, 2022.

[26] Y. Li, M. R. Krisshnamurthi, W. Luo, A. K. Swan, X. Ling, and R. Paiella, "Graphene metasurfaces for terahertz wavefront shaping and light emission [Invited]," Optical Material Express, vol.12, no.12, p.4528, 2022.

[27] C. Shi, I. J. Luxmoore, and G. R. Nash, "Gate tunable graphene-integrated metasurface modulator for mid-infrared beam steering," Optical Material Express, vol.27, no.10, p.14577, 2019.

[28] S. Yu, Y. Kim, E. Shin, and S. H. Kwon, "Dynamic Beam Steering and Focusing Graphene Metasurface Mirror Based on Fermi Energy Control," Micromachines, vol. 14, no. 4, p. 715, 2023.

[29] Z. Li, K. Yao, F. Xia, S. Shen, J. Tian, and Y. Liu, "Graphene Plasmonic Metasurfaces to Steer Infrared Light," Scientific Reports, vol. 5, no. 1, 2015.

[30] B. Zheng, X. Rao, Y. Shan, C. Yu, J. Zhang, and N. Li, "Multiple-Beam Steering Using Graphene-Based Coding Metasurfaces," Micromachines, vol. 14, no. 5, p. 1018, 2023.

[31] P. Das, “Beam-steering of THz MIMO antenna using graphene-based intelligent reflective surface,” Optical and Quantum Electronics, vol. 55, no. 8, 2023.

[32] C. Wang, X. Li, H. Chu, B. Liu, S. Miao, R. Peng, M. Wang, and Yun Lai, “Programmable flip-metasurface with dynamically tunable reflection and broadband undistorted transmission,” Nanophotonics, vol. 13, no. 12, pp. 2151–2159, 2024.

[33] F. Jabbarzadeh, M. Heydari, and A. Habibzadeh-Sharif, “A comparative analysis of the accuracy of Kubo formulations for graphene plasmonics,” Materials Research Express, vol.6, no. 8, p.086209, 2019.

[34] H. Zhang and Z. Wu, “Analysis of Electromagnetic Properties of New Graphene Partial Discharge Sensor Electrode Plate Material,” Sensors, vol.22, no.7, p.2550, 2022.

[35] A. S. Vorobev, G. V. Bianco, G. Bruno, A. D’Orazio, L. O’Faolain, and M. Grande, “Tuning of Graphene-Based Optical Devices Operating in the Near-Infrared,” Applied science letters., vol.11, no.18, p.8367, 2021.

[36] T. Yatooshi, A. Ishikawa, and K. Tsuruta, “Terahertz wavefront control by tunable metasurface made of graphene ribbons,” Applied Physics Letters, vol. 107, no. 5, 2015.

[37] C. A. Balanis, “Antenna Theory Analysis and Design,” John Wiley & Sons, fourth edition, 2016.

[38] D. Chen, J. Yang, J. Huang, Z. Zhang, W. Xie, X. Jiang, X. He, Y. Han, Z. Zhang, and Y. Yu, “Continuously tunable metasurfaces controlled by single electrode uniform bias-voltage based on nonuniform periodic rectangular graphene arrays,” Optics Express, vol. 28, no. 20, p. 29306, 2020.

[39] B. Wang, X. Luo, Y. Lu, and G. Li, “Full 360° Terahertz Dynamic Phase Modulation Based on Doubly Resonant Graphene–Metal Hybrid Metasurfaces,” Nanomaterials, vol. 11, no. 11, p. 3157, 2021.

[40] H. Ai, Q. Kang, W. Wang, K. Guo, and Z. Guo, “Multi-Beam Steering for 6G Communications Based on Graphene Metasurfaces,” Sensors, vol. 21, no. 14, p. 4784, 2021.

[41] Y. Zhang, Y. Feng, and J. Zhao, “Graphene-Enabled Tunable Phase Gradient Metasurface for Broadband Dispersion Manipulation of Terahertz Wave,” Micromachines, vol. 14, no. 11, p. 2006, 2023.

This page intentionally left blank.